Conference Paper, Published Version

Schanz, Tom; Lins, Y.

Hydraulic-mechanical behavior of partially saturated sand (Hydraulisch-mechanisches Verhalten von teilgesättigtem Sand)

13 Hydraulic-mechanical behavior of partially saturated sand

Hydraulisch-mechanisches Verhalten von teilgesättigtem Sand

T. Schanz & Y. Lins

Professur Bodenmechanik, Bauhaus – Universität Weimar, Weimar
Laboratory of Soil Mechanics, Bauhaus–University Weimar, Weimar, Germany

ABSTRACT: In this study the complex coupled hydraulic-mechanical behavior of partially saturated granular frictional materials ("sand") is examined. The material used in our investigation is the well known French Hostun Sand. To study the behavior of partially saturated sand the capillary pressure saturation relationship (soil water characteristic curve: SWCC) for both dense and loose sand specimen was determined. Suction mode as well as pressure mode procedure (axis translation technique) was applied in a modified pressure plate apparatus. The influence of suction on stiffness behavior was studied by performing one dimensional compression and rebound tests in a modified oedometer cell for loose and dense specimen with different initial matric suction values. Matric suction was maintained constant during loading and unloading paths in these tests. Additionally large scale column tests were carried out for loose and dense specimen to investigate capillary pressure-saturation relationship and unsaturated conductivity. The results of the one dimensional compression and rebound tests showed that there is an influence of suction on the compression behavior of the sand which is manifested on the stiffness modules and the compression index of the material for loading conditions. Capillary pressure-saturation relationships which were derived from modified pressure plate apparatus and large scale column test show significant differences in the results for the loose and the dense specimens. A clear influence of the hydraulic loading path direction (hysteresis) can be observed. This phenomenon was also observed for the results of the relative hydraulic conductivity.

KURZFASSUNG: In diesem Beitrag werden Ergebnisse einer experimentellen Untersuchung zum gekoppelten hydraulisch mechanischen Verhalten von Sand präsentiert. Ein wichtiges Element zur Beschreibung teilgesättigter granularer Reibungsmaterialien ist die Kapillardruck-Sättigungsbeziehung. Sie beschreibt den Zusammenhang zwischen der Saugspannung und dem Wassergehalt bzw. der Sättigung eines Bodens. Ein wesentliches Merkmal ist die Abhängigkeit dieser Beziehung von der Belastungsrichtung (Hysterese), der Belastungsgeschwindigkeit (dynamischer Einfluss auf die Kapillardruck-Sättigungsbeziehung) und dem initialen Zustand (Hauptbe- und Hauptentwässerungskurven versus *Scanning* - Kurven). Des Weiteren werden in diesem Beitrag die relative Permeabilität und die Kompressibilität von Sand in Abhängigkeit von der Saugspannung bzw. der Sättigung ermittelt.

13.1 Introduction

In geotechnical engineering, where mostly unsaturated soils are predominant, the principles and classical concepts of saturated soils are not any more consistent. For many practical geotechnical problems knowledge of the influence of water content on the coupled hydraulic-mechanical behaviour is of major interest, because the amount of water in soils is changing drastically their constitutive behaviour. The most important relation to describe unsaturated soil behaviour is the capillary pressure-saturation curve (SWCC), also known as retention curve in the field of soil science. For granular frictional materials it describes the relationship between the gravimetric water content, degree of saturation or volumetric water content versus matric suction value. Osmotic component of suction is not considered in the following. This relationship is additionally used to determine the unsaturated conductivity of soils. The unsaturated conductivity for one and the same soil, assuming constant state, depends significantly on the suction over a wide range of values. Presence of water is also changing the shear strength */Bishop 1961, Donald 1956/* and volumetric behaviour (stiffness) of a soil. In this study we concentrate on the determination of capillary pressure-saturation relationship, the unsaturated conductivity and the influence of matric suction on stiffness behaviour.

Table 13.1 Properties of Hostun Sand

	Hostun Sand
Specific Gravity ρ_s [g/cm³]	2,65
Coefficient of uniformity C_u	1,50
Coefficient of curvature C_c	1,11
Classification (USCS)	SP

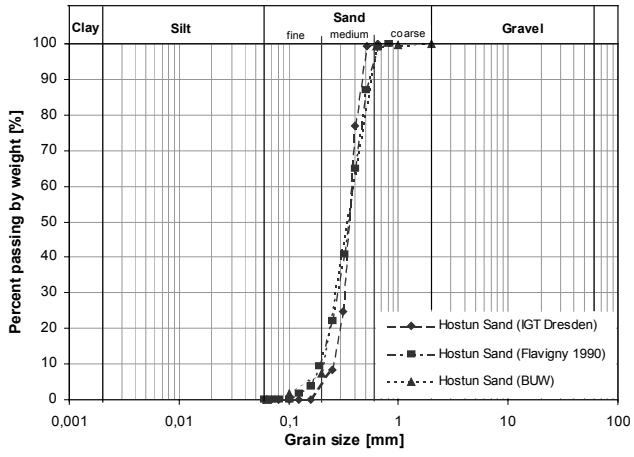

Figure 13.1 Grain size distribution curves of Hostun Sand tested by different laboratories

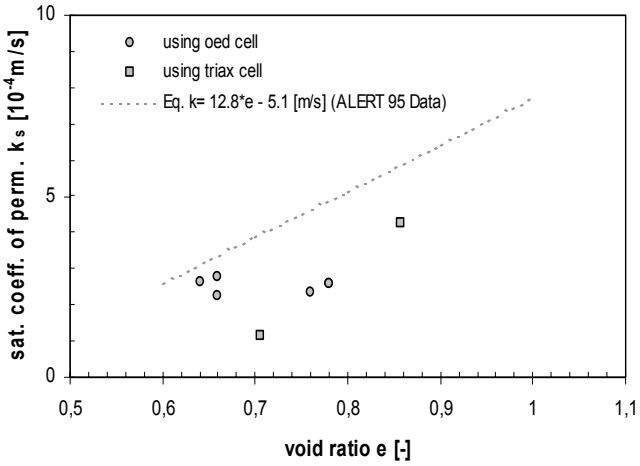

Figure 13.2 Saturated coefficient of permeability as function of void ratio

13.2 Material used

The material used in this study is a quartz sand named Hostun Sand, which is well studied in literature */Flavigny et al. 1990, 1993; Schanz 1998/*. The properties as well as the grain size distribution curve are given in Table 13.1 and Figure 13.1. With a coefficient of uniformity C_c = 1.50 and grain sizes ranging from 0.1 to 1.0 mm the material represents a uniformly graded, medium sand. The coefficient of saturated permeability versus void ratio is given in Fig. 13.2.

13.3 Experimental program

The experimental program consists of the determination of the capillary pressure-saturation relationship, one dimensional compression and rebound tests with different constant suction values as well as large scale column tests. All experiments were done for both loose and dense initial state of specimens. For determining capillary pressure-saturation relationship and performing one dimensional compression and rebound tests a modified pressure plate apparatus and an UPC Controlled-Suction Oedometer Cell were used. Both cells are equipped with a porous stone on the top and a ceramic disc (air entry value of 1 bar) on the bottom. Additionally the equipment is extended with a burette, attached to the water reservoir below the ceramic disc and an air pressure control system connected to the top. Both, pressure plate apparatus tests and one dimensional compression and rebound tests, were carried out for loose as well as for dense states ($e_0 = 0.89 \pm 0.005$ respectively $e_0 = 0.66 \pm 0.005$). Large scale tests were performed in a column (diameter: 30 cm, height: 65 cm), where 6 tensiometers along the vertical axis of the column were measuring the water potential during wetting and drying processes. More detailed information about this testing device is given in section 13.3.3.

13.3.1 Determination of SWCC

Capillary-pressure-saturation relationships were determined for loose and dense specimen as mentioned above. Dry sand specimen were prepared directly into the ring of the cell and saturated in the following step by using the attached burette. Starting from saturated conditions with respect to the fluid (S_r = 1.0) the specimen was drained in a first cycle and wetted afterwards. By lowering down the attached burette (suction mode test) with respect to the top of the ceramic disc small suction values up to ψ = 5 kPa were applied to the specimen. Higher suction up to ψ = 50 kPa was induced by pressure mode test, which means that air overpressure was applied from the top of the specimen. The suction mode test and pressure mode test follow the principle of the axis translation technique according to */Hilf 1956/*. The amounts of water during desorption and adsorption paths were measured in the attached burette with a capacity of 25 cc and a least count of 0.05 cc. After finishing each test, the specimen was dismantled and the gravimetric water content was determined by oven drying. Back calculation method was used to compute volumetric water content θ, the degree of saturation S_r and the gravimetric water content w for each applied matric suction value. Doing so main wetting and drying curves for loose and dense sand specimen were derived.

13.3.2 One dimensional compression and rebound tests with constant suction

One dimensional compression and rebound tests with different constant suction values were carried out for loose and dense specimen. Therefore dry specimens were prepared directly in the UPC Controlled Suction Oedometer Cell. After saturating the specimen the target suction was applied by using suction mode procedure for ψ = 1.5 kPa and ψ = 3.0 kPa and pressure mode procedure for ψ = 20 kPa and ψ = 50 kPa as described above. The specimens were loaded up to 200 kPa net stress and unloaded to 2 kPa. Correction was applied to the measured vertical net stress due to shear stresses between the oedometerring and the soil sample. Both, frictional and cohesional effects were taken into account following */Fredlund 1996/*.

13.3.3 Large scale column tests

As mentioned above large scale tests were performed in a column (diameter: 30 cm, height: 65 cm). A schematic sketch of the set up is given in Figure 13.3. There it is shown that six tensiometers placed in a row along the height of the column are measuring water potential changes during wetting and drying processes. The tensiometers are connected to a data logger system and then to a computer. Two burettes attached at the column are monitoring the rise and fall in water level. A pump connected to the water reservoir at the bottom of the

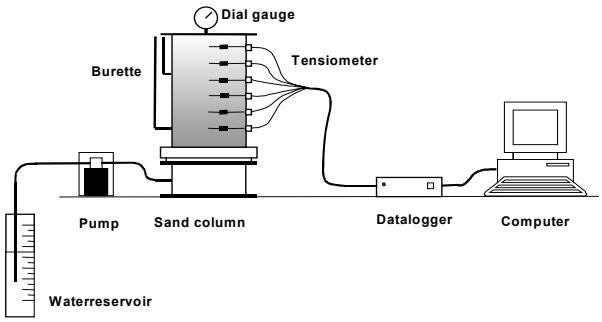

Figure 13.3 Experimental set up of large scale column test

column is pumping water in and out of the specimen with a constant flow rate. Wet loose (e_0 = 0.88, w_0 = 0.08) and dense (e_0 = 0.66, w_0 = 0.16) specimen were prepared in several layers directly in the column. The tests started with a wetting phase followed by a drying one. In total four wetting and drying cycles were performed.

13.4 Experimental results

13.4.1 Capillary-pressure saturation relationship

The capillary pressure-saturation relationship for a loose specimen in comparison with a dense specimen is shown in Fig. 13.4, where volumetric water content is plotted versus matric suction for main drying and wetting cycles. According to */Fredlund 1994/* typical ranges of constitutive behaviour are included into the diagram for the drying cycle, exemplary for the dense specimen. By using Eq. 13-1 from */van Genuchten 1980/* and a least square approach the experimental results were fitted:

$$\Theta = \frac{1}{\left[1+(\alpha\varphi)^n\right]^m} \qquad (13\text{-}1)$$

where Θ is the normalised water content $\Theta = (\theta - \theta_r)/(\theta_s - \theta_r)$ with θ_r = residual water content and θ_s = saturated water content, φ is the suction value and α, n, m are constants.

Insignificant volume changes were measured during the wetting and drying phases.

Hysteresis is very significant for this loading path:

- With a value of ψ_{AEV} = 2.0 kPa the dense specimen shows a slightly higher air entry value (AEV) then the loose specimen, ψ_{AEV} = 1.5 kPa.
- When reaching the air entry value the water content is decreasing in a small range of suction for both sand samples. This zone, the so-called transition zone, is between

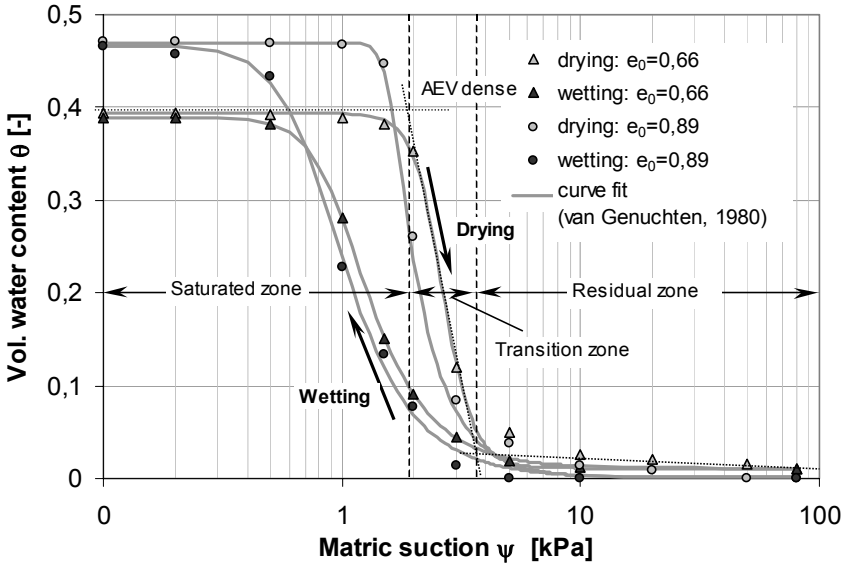

Figure 13.4 SWCC 1: volumetric water content versus matric suction

2.0 kPa to 4.0 kPa for the dense specimen and between 1.5 kPa and 4.0 kPa for the loose specimen.

- The residual zone starts at low suction value for the drying cycle for dense as well as for loose specimen.
- During wetting no significant changes in water content were observed in a range of 50.0 kPa to 3.0 kPa. The transition zone starts for dense specimen at the water entry value of about ψ_{WEV} = 0.7 kPa and for the loose specimen at ψ_{WEV} = 0.4 kPa. It ends for both states at nearly 3.0 kPa.
- The saturated zone falls in a very narrow range of 0.7 kPa to 3.0 kPa for the dense specimen and 0.4 kPa to 3.0 kPa for the loose specimen.

Typical observations with increasing initial density are (see also Fig. 13.5):

- Decreasing water content *w* for saturated condition S_r = 1.0
- Decreasing hysteresis
- Slightly higher air entry value
- Slightly higher water entry value

The model of */Mualem 1976/* in connection with the calculated van Genuchten parameter *m,* applying the relation *m*=1-1/*n*, was used for predicting the relative hydraulic conductivity k_r for the wetting phase of the dense and loose specimen:

$$k_r\left(S_e\right) = S_e^l\left[1-\left(1-S_e^{1/m}\right)^m\right]^2 \qquad (13\text{-}2)$$

where k_r is relative hydraulic conductivity, S_e is the effective saturation, *m* is van Genuchten parameter taken from curve fitting of the capillary pressure saturation – relationship and *l* is a pore conductivity parameter. This pore conductivity parameter *l* was estimated by */Mualem 1976/* to be 0.5 as an average value for most soils. Results are given in Fig. 13.6. In this diagram relative hydraulic conductivity is plotted versus effective saturation. The unsaturated conductivity was calculated from the following relationship */Lu, Likos 2004/*:

$$k_r = \frac{k_w}{k_s} \qquad (13\text{-}3)$$

with k_r relative hydraulic conductivity, k_w unsaturated conductivity and k_s saturated hydraulic conductivity. For the dense specimen k_s = 0.0278 cm/s and for the loose specimen k_s = 0.0275 cm/s was used. The relative hydraulic conductivity versus matric suction is plotted in Fig. 13.7. Comparing the curves of the loose and dense specimen for the drying cycle one can see that the dense drying curve results in higher relative hydraulic conductivity values. The capillary pressure-saturation curve is related to the hydraulic conductivity and this is the reason why both, the main drying and main wetting cycle of the loose and dense specimen show hysteresis, too. In Fig. 13.8 the hysteresis is very clearly shown. The unsaturated conductivity of the dense specimen is larger than for the loose specimen for the drying path as well as for the wetting path. For instance at matric suction of ψ = 2.2 kPa for the dense specimen at drying path an unsaturated conductivity of k_w = 0.0113 cm/s was calculated and for the loose specimen k_w = 0.0023 cm/s was calculated. At matric suction ψ = 0 kPa (water saturated condition: S_r = 1.0) one can read k_w = 0.0264 cm/s for the dense specimen and k_w = 0.0275 cm/s for the loose specimen, which are equal to the saturated conductivity values. Unsaturated conductivity is only decreasing slightly

till reaching the air entry value. After reaching the air entry value the unsaturated conductivity decreases rapidly, because the amount of water is decreasing drastically due to the relatively large and uniform pores of the material and because the path where water can flow becomes smaller and more tortuous. At high matric suction values (residual zone), where water is only present as a thin layer on the skin of the sand grains the unsaturated conductivity is reaching zero value.

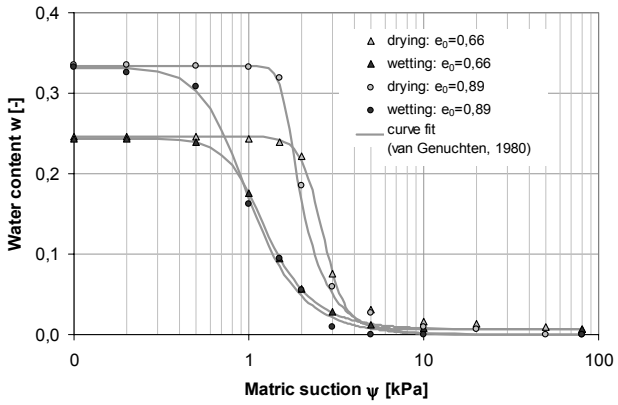

Figure 13.5 SWCC 2: water content versus matric suction

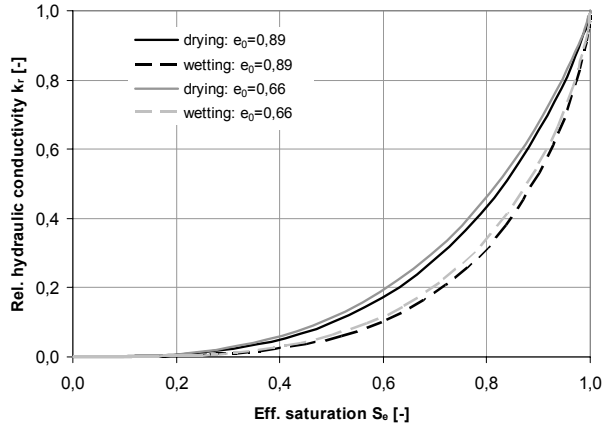

Figure 13.6 Relative hydraulic conductivity versus effective saturation from pressure plate

13.4.2 Results from one dimensional compression and rebound test with constant suction

To study the influence of matric suction on the volumetric behaviour of sand, oedometer tests with constant suction were carried out. These results from one dimensional compression and rebound tests are given in Fig. 13.9 where void ratio change resulting from change of vertical net stress is displayed. As a third dimension suction is included in Fig. 13.10a &b.

From these figures one can see that as anticipated the stiffness of the dense specimen is higher then for the loose specimen for the same suction. Test carried out for dense specimen show that the stiffness increases with matric suction from 1.5 kPa, 3.0 kPa and 20.0 kPa. For the test with matric suction of 50 kPa lowest stiffness was calculated. The unloading behaviour of both, dense and loose specimen is similarly and independent of applied suction. To further underline the observed behaviour in Fig. 13.11 compression and swelling index are displayed. No influence of the suction on the swelling index can be observed. Stress dependent stiffness moduli */Ohde 1939, Schanz 2002/* were calculated for vertical net stresses σ^* of 12 and 100 kPa from Eqs. 13-4 and 13.5, where E_{oed} is the normalized stiffness modulus for initial loading and E_{ur} is the normalized stiffness modulus for un-/reloading path:

$$E_{oed} = E_{oed}^{ref}\left(\frac{\sigma^*}{\sigma_{ref}^*}\right)^m : \sigma_{ref}^* = 100kPa \qquad (13\text{-}4)$$

$$E_{ur} = E_{ur}^{ref}\left(\frac{\sigma^*}{\sigma_{ref}^*}\right)^m : \sigma_{ref}^* = 100kPa \qquad (13\text{-}5)$$

m for the dense specimen was derived in a range of 0.62 to 0.81 and for the loose specimen from 0.53 to 0.73.Table 13.2 gives the detailed results.

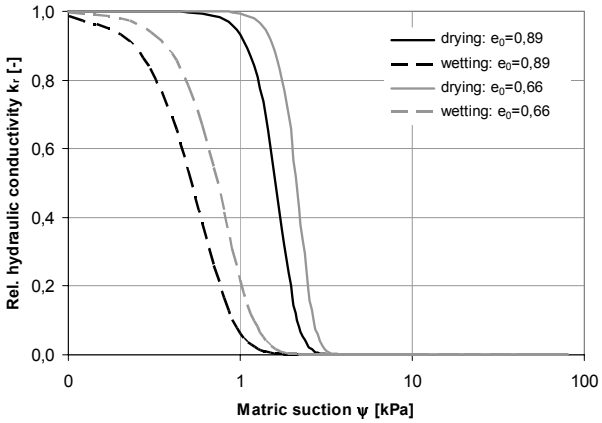

Figure 13.7 Relative hydraulic conductivity versus matric suction from pressure plate

13.4.3 Results from large scale test

Large scale column test with four wetting and drying cycles were performed under laboratory conditions. During the wetting and drying processes 6 tensiometers placed along the column were measuring the changes in hydraulic potential. As an example for one drying process (cycle 1) the tensiometers readings are plotted in Fig. 13.12 (loose initial state). With an initial value of about 50 cm the tensiometer T1 is located at the bottom of the saturated sand column. Tensiometer T6 measures a value of -3 cm. The value of -3 cm indicates a matric suction of ψ = 0.3 kPa at the top of

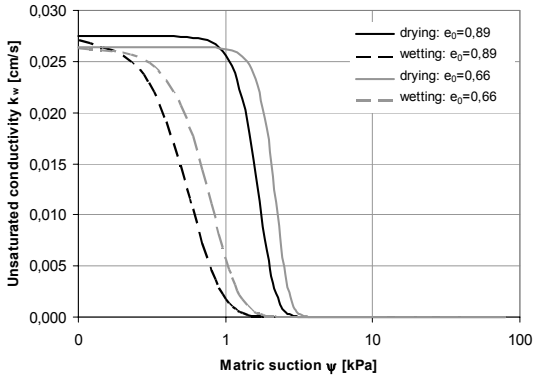

Figure 13.8 Unsaturated conductivity versus matric suction from pressure plate

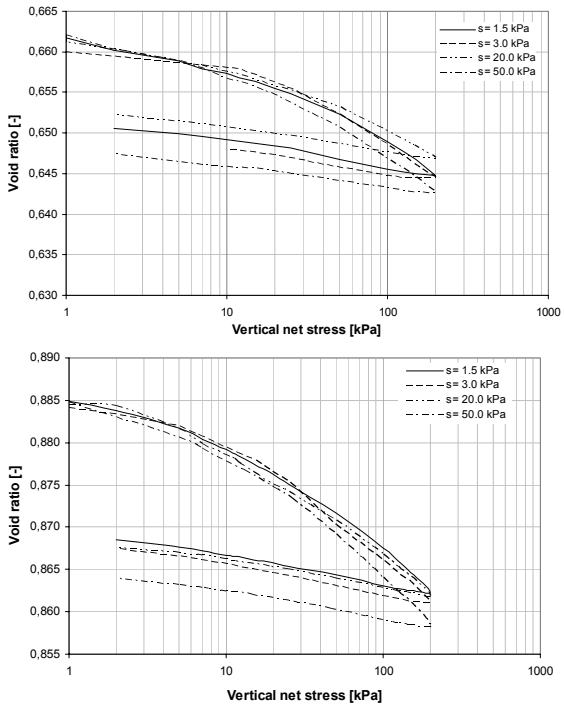

Figure 13.9 Vertical net stress versus void ratio for dense (top) and loose (bottom) specimen under oedometer loading conditions

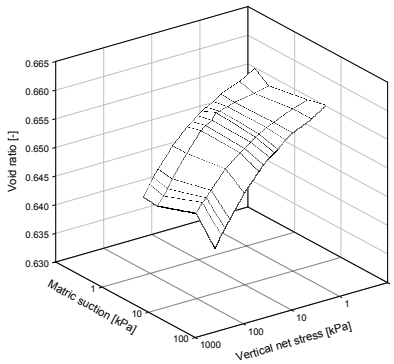

Figure 13.10a State surface from oedometer test results for dense specimen

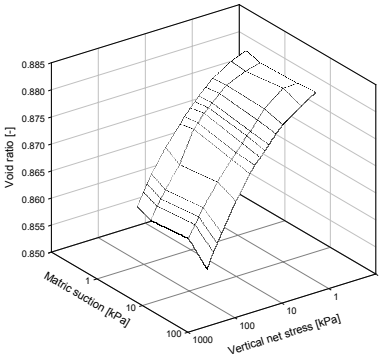

Figure 13.10b State surface from oedometer test results for loose specimen

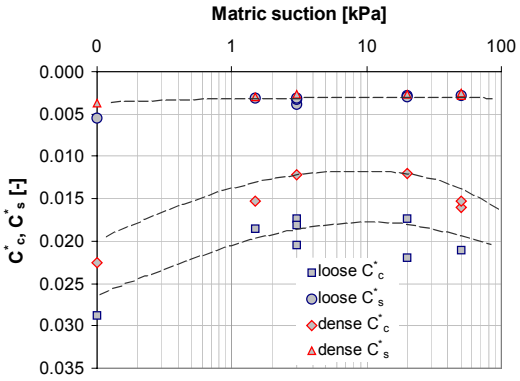

Figure 13.11 Compression and swelling index versus suction for loose and dense initial state

Table 13.2 Stiffness modules (MPa) from oedometer

Matric suction [kPa]	dry	1.5	3.0	20.0	50.0
dense					
E_{oed} σ^* =100	23.3	30.0	29.4	35.6	27.8
E_{oed} σ^* =12	10.4	6.9	8.2	8.1	5.7
E_{ur} σ^* =100	175.2	131.5	258.0	141.3	167.8
E_{ur} σ^* =12	8.0	14.8	10.4	15.9	16.3
loose					
E_{oed} σ^* =100	15.1	24.4	24.7	24.6	22.8
E_{oed} σ^* =12	6.7	6.6	7.1	5.4	4.9
E_{ur} σ^* =100	102.9	154.9	138.3	125.7	153.8
E_{ur} σ^* =12	7.6	15.0	12.0	17.2	17.0

the column, which is negligible small. In Fig. 13.13 tensiometer readings of one wetting phase (cycle 3, dense initial state) are shown. The initial potential of about –43 cm corresponds to a matric suction of ψ = 4.3 kPa. Taking into account Fig. 13.4, where volumetric water content is plotted versus matric suction, one can see that the state of the specimen falls into the residual zone. While tensiometer 1 (bottom of the specimen) shows a smooth transition from unsaturated condition to saturated condition, the curve shape of the tensiometers T3, T4 and T5

show a significant “sharp” wetting front. This kind of wetting front we could observe during all wetting cycles. No transient unsaturated zone for calculating unsaturated conductivity was observed to occur. Obviously the applied flow rate of 24 ml/min was too high. That is why only the drying process of one loose and one dense specimen is further investigated. In the next step we applied an inverse approach utilizing the HYDRUS 1D code to determine the van Genuchten parameters *a*, *n* and *m* from the measurements of the column tests (Tab. 13.3). The capillary pressure – saturation relationship of the loose and dense specimen is given in Fig. 13.14. For loose specimen an air entry value of ψ_{AEV} = 2.2 kPa and for the dense specimen an air entry value of ψ_{AEV} = 3.0 kPa was found.

Table 13.3 Van Genuchten parameters for loose and dense specimen from inverse modelling of large scale column test

	van Genuchten - parameters		
	a	n	m=1-1/n
loose	0.3036	4.2270	0.7634
dense	0.2192	5.1070	0.8042

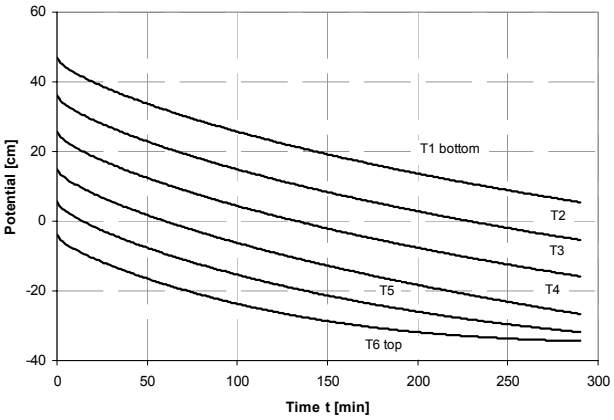

Figure 13.12 Tensiometer readings of drying process for loose sand specimen from column test

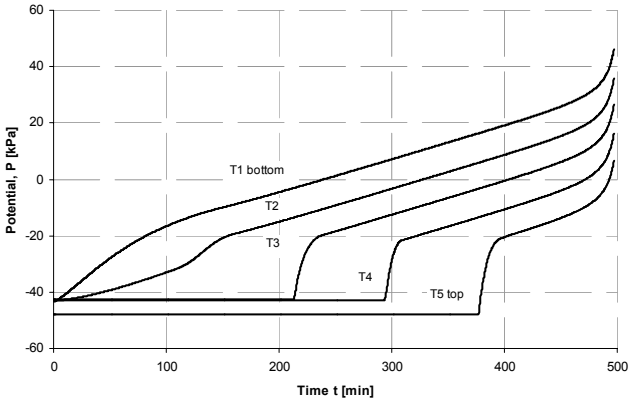

Figure 13.13 Tensiometer readings of wetting process for dense sand specimen from column test

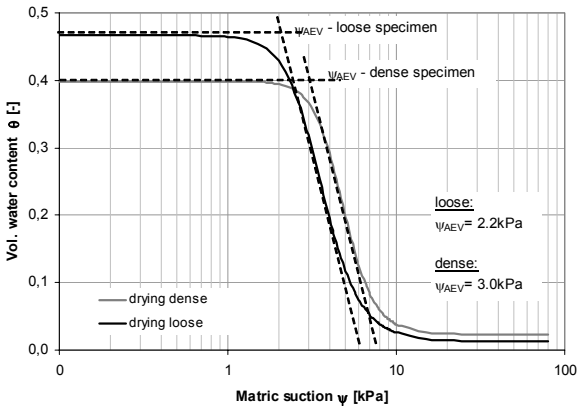

Figure 13.14 Volumetric water content versus matric suction of dense and loose specimen: drying cycle from column test

By using the results from Fig. 13.2 the relative hydraulic conductivity as well as the unsaturated conductivity was calculated. These results are given in Figs. 13.15 and 13.16. The results from the sand column test show the same qualitative behaviour as the results from the pressure plate apparatus. The relative hydraulic conductivity/ unsaturated conductivity is larger for the dense specimen than for the loose specimen.

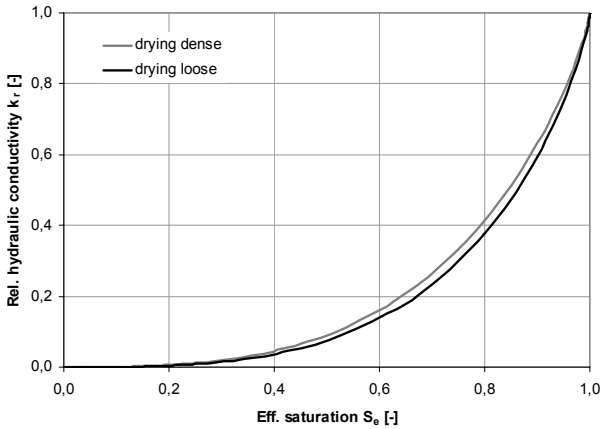

Figure 13.15 Relative hydraulic conductivity versus effective saturation for dense and loose specimen from column test

13.4.4 Comparison of the results from modified pressure plate apparatus and large scale column test

The primary reason for conducting the column tests was to compare the influence of boundary and initial conditions on the coupled hydraulic/mechanical behaviour. Comparing with results from the modified pressure plate we found significant differences for the SWCC and therefore for the relative conductivity function. In Fig. 13.17 the capillary pressure-saturation relationship calculated from modified

pressure plate apparatus is compared to the one from the large scale column test. One can observe that the curves calculated from large scale column tests are shifted to the right to higher suction values. The air entry value of the dense specimen is for instance shifted from ψ_{AEV} = 2.0 kPa for the results taken from modified pressure plate apparatus to ψ_{AEV} = 3.0 kPa for the results from large scale column test. Additionally one can observe that the curves calculated from the large column generally show a flatter shape.

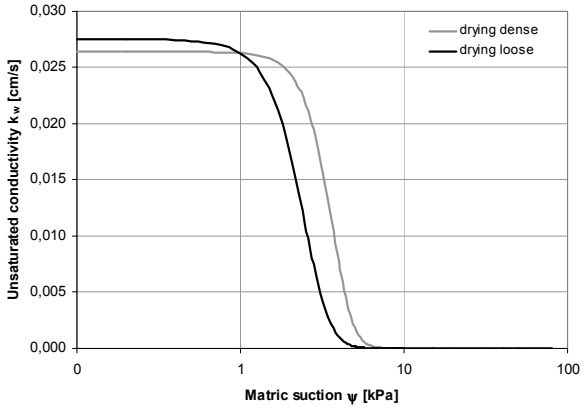

Figure 13.16 Unsaturated conductivity versus matric suction for dense and loose specimen from column test

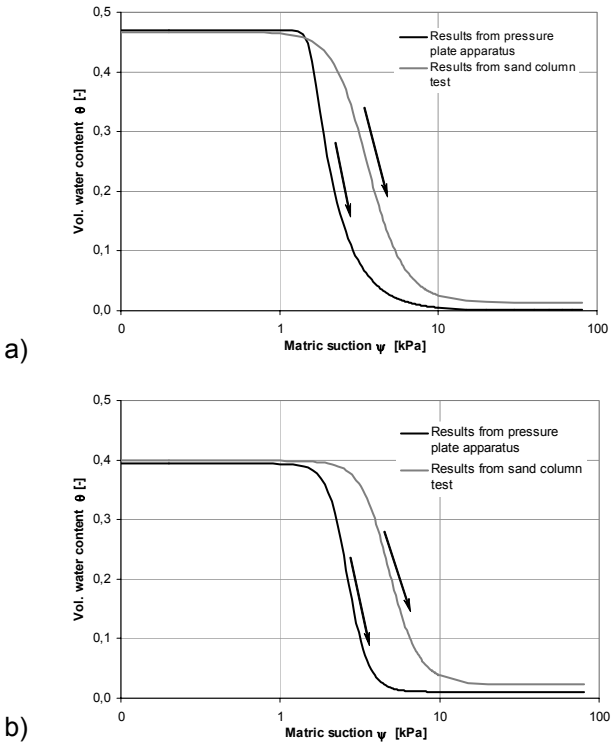

Figure 13.17 Comparison of SWCC calculated from modified pressure plate apparatus and large scale column test for a) loose and b) dense specimen

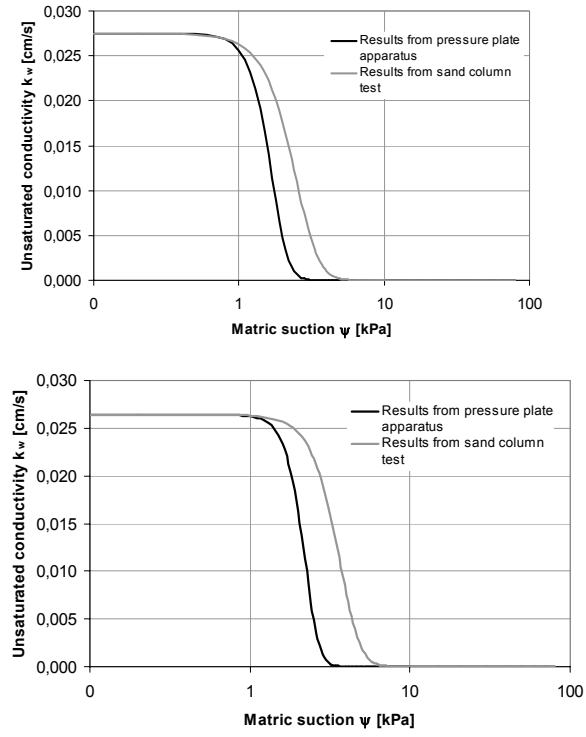

Figure 13.18 Comparison of unsaturated conductivity calculated from modified pressure plate apparatus and large scale column test for a) loose specimen and b) dense specimen

So the van Genuchten parameter *n*, which is responsible for the slope of the curve, is with *n* = 7.14 for the results from modified pressure plate apparatus higher than *n* = 5.12 for the results from large scale column test (dense specimen). As smaller *n* as flatter the slope of the curve. With the difference in the shape of the capillary pressure-saturation relationship curves and the resulting different parameters the unsaturated conductivity differs between the results from the pressure mode test and the large scale column test, too.

These results are given in Fig. 13.18. The unsaturated conductivity is larger following the large scale column test than following the results taken from the modified pressure plate apparatus.

The dependency of loading history and loading direction on the SWCC (wetting or drying path) is well known (hysteresis, see Fig 13.4 or 13.5). Much less recognized is the dynamic effect caused by the applied rate of change of saturation */Hassanizadeh et al. 2002/*. Based on thermodynamic considerations the well known definition of capillary pressure $s = u_a - u_w$ */Bear & Verruijt 1987/* was extended by a dynamic part */Hassanizadeh & Gray 1993/*:

$$u_a - u_w - s(S_r) = -\tau(S_r)\frac{\partial S_r}{\partial t} \tag{13-6}$$

where u_a is air pressure, u_w is water pressure, S_r is saturation, s is capillary pressure and τ an additional

dynamic coefficient. In general capillary pressure-saturation curves can be determined by one of the following methods:

- Static equilibrium method
- Unsteady state method

In the static equilibrium method different values of suction are applied to the specimen, each individual step waiting until equilibrium is reached (see 13.3.1). For the unsteady state method a "large" change of suction is applied to the specimen, causing transient change of water content. This transient state is analyzed further, as for example in the column test. In */Hassanizadeh et al. 2002/* it is shown, that, for the same saturation, suction resulting from unsteady state method is higher than the one from the steady state method. This is what we found in our investigations.

13.5 Conclusion

Summarizing the results from our experimental study we can draw the following conclusions:

The capillary pressure-saturation relation shows a significant hysteretic behaviour for loose and dense specimen. This hysteresis was also found for unsaturated conductivity.

Stiffness for one dimensional compression is clearly influenced by suction for the case of initial loading.

Comparing results from column test and modified pressure plate apparatus reveals the influence of dynamic effects on the hydraulic behaviour.

To take into consideration these findings we will improve the testing procedure in the large scale column in the future: We will measure both the hydraulic potential as well as the water content versus time in order to calculate the dynamic coefficient τ, which is describing the difference between the curves determined under static equilibrium method and unsteady state method.

13.6 Acknowledgements

The authors acknowledge Deutsche Forschungsgemeinschaft (DFG) for the support in the frame of the research group "Mechanik teilgesättigter Böden" (FOR 444).

13.7 Literatur

Bishop, A.W. &. Donald, I.B. (1961)

The experimental study of partially saturated soil in the triaxial apparatus. In: Proceedings of the 5th Int. Conf. Soil Mech., Paris, France, 13-22

Donald, I.B. (1956)

Shear strength measurements in unsaturated non-cohesive soils with negative pore pressures. In: 2nd Australie-New Zealand Conf. Soil Mech. Found. Eng., Christchurch, New Zealand, 200-205

Flavigny, E. et al. 1993

Compalition des essais triaxiaux de revolution sur le sable d'Hostun RF. In: Internal Report IMG, Grenoble

Flavigny, E., Desrues J. and Palayer 1990

Note technique: Le sable d'Hostun RF. Rev. France. Géotech. 53, 67-70

Fredlund, D.G. &. Xing, A. 1994

Equations for the soil-water characteristic curve. Can. Geotech. J. 31, 4, 521-532

Fredlund, D.G., Xing, A., Fredlund, M.D. & Barbour, S.L. 1996

The relationship of the unsaturated soil shear strength to the soil water characteristic curve. Can. Geotech. J. 33, 4, 440-448

van Genuchten, M.Th. 1980

A closed-form equation for predicting the hydraulic conductivity of unsaturated soils. Soil Sci. Soc. Am. J., Vol. 44, 892-898

Hassanizadeh,S.M., Celia, M.A. & Dahle, H.K. 2002

Dynamic effect in the capillary pressure-saturation relationship and ist impacts on unsaturated flow. Vadouse Zone Journal 1, 38-57

Hassanizadeh, S.M. & Gray, W.G. (1993)

Thermodynamic basis of capillary pressure in porous media. Water Resour. Res. 29, 3389-3405

Hilf, J.W. 1956

An investigation of pore-water pressure in compacted cohesive soils. PhD dissertation, Technical memo No. 654, U.S. Departement of interior, Bureau of reclamation, Design and construction division, Denver, Colorado

Lu, N. & Likos W.J. 2004

Unsaturated soil mechanics. John Wiley & Sons, Inc., Hoboken, New Jersey

Mualem, Y. 1976

A new model for predicting the hydraulic conductivity of unsaturated porous media. Water Resour. Res.., 12(3), 513-522

Ohde, J. 1939

Zur Theorie der Druckverteilung im Baugrund. Bauingenieur, No. 20, 451-459

Schanz, T. 1998

Zur Modellierung des mechanischen Verhaltens von Reibungsmaterialien. In: Institut für Geotechnik, Universität Stuttgart, Heft 45